INDOOR TIME REVERSAL WIRELESS COMMUNICATION: EXPERIMENTAL RESULTS FOR LOCALIZATION AND SIGNAL COVERAGE

George C. Alexandropoulos[1], *Ramin Khayatzadeh*[2], *Mohamed Kamoun*[2], *Yang Ganghua*[2], *and Mérouane Debbah*[2]

[1]Dept. of Informatics and Telecommunications, National and Kapodistrian University of Athens, Greece
email: alexandg@di.uoa.gr
[2]Mathematical and Algorithmic Sciences Lab, Huawei Technologies France SASU, France
emails: firstname.lastname@huawei.com

ABSTRACT

Communication based on Time Reversal (TR) exploits rich multipath radio propagation for high resolution spatiotemporal focusing. It refers to the process of transmitting a received signal in a time reversed order, profiting from channel's spatial reciprocity. Recent theoretical studies have shown that signal processing techniques for TR communication have the potential of realizing the benefits of massive antenna systems using only a single antenna base station and simple receive processing circuitry. In addition, TR can offer highly accurate localization, especially when considered for indoor wireless positioning systems. Particularly, the larger the transmission power and bandwidth are, the more observable are the multiple channel paths, hence, TR capability for localization becomes more profitable. In this paper, we implement TR wireless communication at 3.5GHz using up to 600MHz bandwidth channel sounding signals. We present extensive experimental results showcasing the concept's potential for indoor cm-level localization and signal coverage extension.

Index Terms— Coverage extension, positioning, spatiotemporal focusing, time reversal, wideband transmission.

1. INTRODUCTION

Although consensus on the general requirements for fifth Generation (5G) mobile communication networks has been early reached [1, 2], only recently the definition of the 5G use cases together with their key requirements has been finalized. The 5G New Radio (NR) technology [3] includes the uses cases of enhanced mobile broadband, massive machine type communications, as well as ultra-reliable and low latency communications, which have diverging requirements. Emerging wireless applications (like virtual reality and industrial internet of things) falling under the latter use cases have lately paved the way for the highly demanding requirements of beyond 5G communications [4]. Among those requirements belong the cm-level indoor localization accuracy and the necessity for increased indoor signal coverage.

Time Reversal (TR) is a well known signal processing technique [5] that has been lately considered for addressing some of the requirements for 5G, and beyond, communication. In [6], it was advocated that TR communication has the potential of realizing the benefits of massive antenna systems using only a single antenna base station and simple receive processing circuitry. According to TR, radio waves are focused onto a source by emitting a time reversed version of the received wave field measured by a transmitter. The TR refocusing property is due to the channel reciprocity in space and reversability in time for the wave field. The TR spatiotemporal focusing inside a cavity with a 2.45GHz electromagnetic pulse was firstly demonstrated in [7]. In [8], TR for per path pulse distortion was considered in multiuser ultrawideband communications. The temporal focusing and increase in received energy with the number of antennas has been experimentally verified with multi-antenna ultra wideband TR communication [9, 10]. The concept of TR division multiple access was introduced in [11] for multiuser communication.

In this paper, we demonstrate in a laboratory environment TR wireless communication at 3.5GHz using up to 600MHz bandwidth channel sounding signals. We present experimental results showcasing the technique's potential for indoor cm-level localization and signal coverage extension.

2. TIME REVERSAL BASIC THEORY

Wireless communication based on TR consists of two distinct phases: the phase for estimating the Channel Impulse Response (CIR) and the transmission phase. In the CIR estimation phase, a channel sounding signal is sent from the one communication side to the other. Suppose this signal is represented by $s(t)$ and initially transmitted by node $\mathcal{A}$ to the receiving node $\mathcal{B}$. Neglecting the noise term, the received signal

During the preparation of this work Prof. G. C. Alexandropoulos was with the the Mathematical and Algorithmic Sciences Lab, Huawei Technologies France SASU, France.

at node $\mathcal{B}$ can be obtained from the following convolution:

$$y(t) \triangleq s(t) * h(t), \quad (1)$$

where $h(t)$ denotes the CIR between the single-antenna nodes $\mathcal{A}$ and $\mathcal{B}$. Equation (1) represents the CIR estimation phase by node $\mathcal{B}$. Then, this node time reverses $y(t)$ computing $y_{\mathrm{tr}}(t) \triangleq s(-t) * h(-t)$. The time reversed signal $y_{\mathrm{tr}}(t)$ is sent through the same channel from node $\mathcal{B}$ to $\mathcal{A}$, that now has the role of the receiver. Note that, due to the channel's spatial reciprocity, the channel is the same for both directions. The received signal at node $\mathcal{A}$ can be derived as follows:

$$r(t) \triangleq y_{\mathrm{tr}}(t) * h(t) = s(-t) * h(-t) * h(t). \quad (2)$$

It can be easily observed from (2) that the convolution $h(-t) * h(t)$ is obtained from the autocorrelation function of of the CIR $h(t)$. This indicates that when, increasing the randomness of the channel, the peak of the autocorrelation function gets a larger value, which means that the received signal at node $\mathcal{A}$ has larger power. In other words, more multipath in the wireless channel translate to sharper spatiotemporal focusing for the TR technique.

3. TIME REVERSAL EXPERIMENTATION

The real-time experimentation setup for the TR spatial and temporal focusing is demonstrated in Fig.(1). We have considered one TX and two receivers RX_1 and RX_2 inside a 8m×5m laboratory room including various hardware instrumentation, desktop computers, and furniture. The distance between the receivers and TX was around 2m, while we considered various relative distances between RX_1 and RX_2 ranging from 2cm up to 30cm. The transmitting power was set to 10dBm, and the Signal-to-Noise Ratio (SNR) varied between 10dB and 15dB depending on the position of the board where RX_1 and RX_2 were attached to.

As described in Section 2, TR communication from TX terminal to RX_1 (or RX_2) terminal necessitates knowledge of the reciprocal channel from RX_1 to TX in order to time reverse it. In the experimentation setup of Fig.(1), we assume that in a first step channel sounding signals are sequentially sent from TX to RX_1 and RX_2 in order to estimate the CIRs $h_1(t)$ and $h_2(t)$, respectively. The training signal used for channel estimation was the Zadoff-Chu sequence [12] having variable BandWidth (BW) ranging from 20MHz to 600MHz. The training signal in baseband at TX is upconverted to the RF frequency of 3.5GHz using an Arbitrary Waveform Generator (AWG), and the resulting RF signal is transmitted first to RX_1 and then to RX_2. At each receiver side, the received RF signal is amplified using a Low Noise Amplifier (LNA), and then sampled using the National Instruments (NI PXIe 5186) RF acquisition board. The sampled received RF signal is then frequency downconverted and downsampled to baseband using NI's LABView program. The baseband detected signal, via cross correlation with the known at the receivers training signal, is finally used to estimate the CIR from the point of view of each receiver. Each CIR estimation is time reversed and stored on AWG. At a second step, the time reversed signals are sent from TX to RX_1 and RX_2 and the CIRs from the receivers points of view are measured.

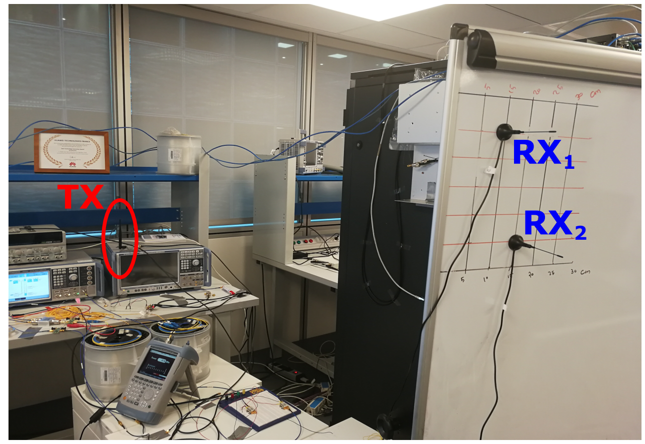

Fig. 1. Time reversal experimentation setup at Huawei Paris Research Center. Various hardware instrumentation, desktop computers, and furniture are present into the 8m×5m laboratory room. RX_1 and RX_2 were placed around 2m far apart from TX. The varying relative distance between RX_1 and RX_2 ranged between 2cm and 30cm.

4. SPATIOTEMPORAL FOCUSING RESULTS

In this section, we present experimental results for the CIR estimation and the cross correlation function between the transmitted and received signals considering different values for the training signal bandwidth. From our extensive measurement campaign, we have found that TR benefits start becoming apparent when the channel has at least 10 significant multipath components. This value relates to the channel's delay spread, which provides a measure of its multipath richness.

4.1. Channel Impulse Response (CIR) Estimation

The CIR estimation between TX and RX_1, as described in Section 3, using channel sounding signals with bandwidths 50MHz, 100MHz, and 200MHz is illustrated in Fig.2. We actully plot CIR's magnitude over time steps; the time steps resolution is fixed to 3.33nsec corresponding to the largest bandwidth value used for sounding signal. As shown in this figure, increasing the bandwidth of the training signal increases the resolution capability of the estimation process. Clearly, the larger bandwidth used, the more multipath richness is unveiled in the estimation. Note that the level of multipath richness is an inherit characteristic of the channel. Increasing the

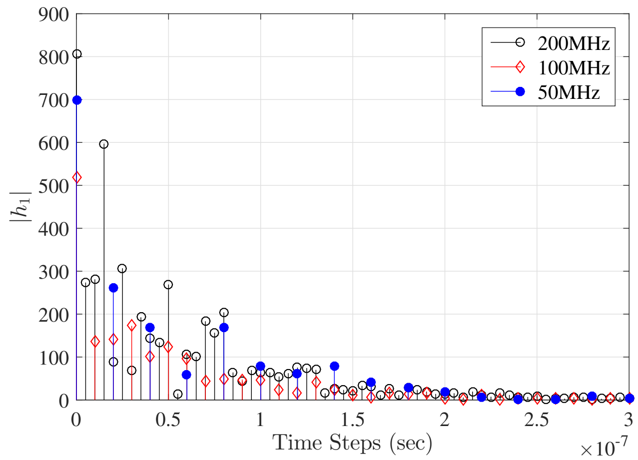

Fig. 2. Estimation of the impulse response of the wireless channel between TX and RX_1 using channel sounding signals with bandwidths 50MHz, 100MHz, and 200MHz.

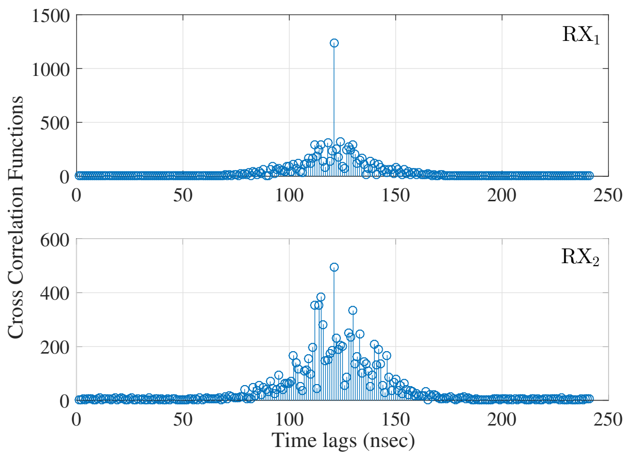

Fig. 3. Cross correlation functions between the transmitted and each of the received signals, when TR is applied to RX_1 using a 200MHz sounding signal.

channel sounding bandwith results in improved time resolution, but cannot have a significant impact on a poor in multipath channel. As it will be shown in the results that follow, TR directly depends on the multipath richness necessitating large bandwith for CIR estimation.

4.2. Cross Correlation Function

The cross correlation function between two discrete signals $x[n]$ and $y[n]$, where $n = 0, 1, \ldots$, is defined as

$$\mathcal{R}[n] \triangleq \sum_{m=-\infty}^{\infty} x^*[m]y[m+n]. \tag{3}$$

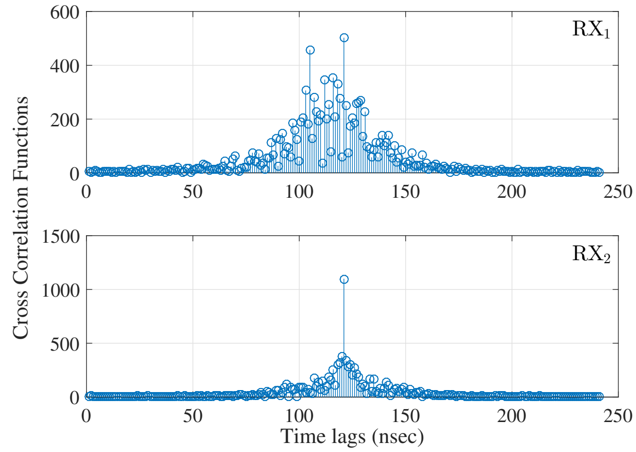

Fig. 4. Cross correlation functions between the transmitted and each of the received signals when TR is applied to RX_2 using a 300MHz sounding signal.

We have set the distance between RX_1 and RX_2 to 5cm and obtained results in Figs. 3 and 4 for the cross correlation function between the transmitted and received signals. Particularly, CIR estimation with a 200MHz sounding signal and TR for RX_1 is considered in Fig. 3, whereas in Fig. 4 we have applied TR for RX_2 using a 300MHz sounding signal. It can be seen from both figures that TR modulation is capable to significantly increase the main path's amplitude value compared to the weaker channel paths. For example, after applying TR to RX_1 in Fig. 3 for 200MHz, the main path's amplitude is increased to around 1300, while for RX_2 this value is around 500. Approximately the same results have been collected after applying TR to RX_2 for 300MHz, as depicted in Fig. 4. The latter results for 5cm distance between RX_1 and RX_2 indicate that TR has the potential of serving as a very precise tool for indoor localization purposes.

Considering the same 5cm distance between RX_1 and RX_2, we proceed by investigating the CIR estimation resolution on TR's spatiotemporal performance. More specifically, we apply TR to RX_1 using a relative small bandwidth value for the training signal and a much larger one. Figure 5 illustrates the cross correlation function of the training signal with 34MHz bandwidth before and after applying TR. As can be observed from this figure, TR is incapable of increasing the amplitude of the main channel path compare to the weaker ones. In fact, the values for the cross correlation function with and without TR nearly coincide. This trend confirms that the TR performance strongly depends on the CIR estimation resolution. In Fig. 6, we have increased the training signal's bandwidth to 138MHz, and as illustrated, the amplitude of the main channel path compared to the weaker ones is significantly increased when TR is applied. Putting all above together, we conclude that TR can provide cm-level

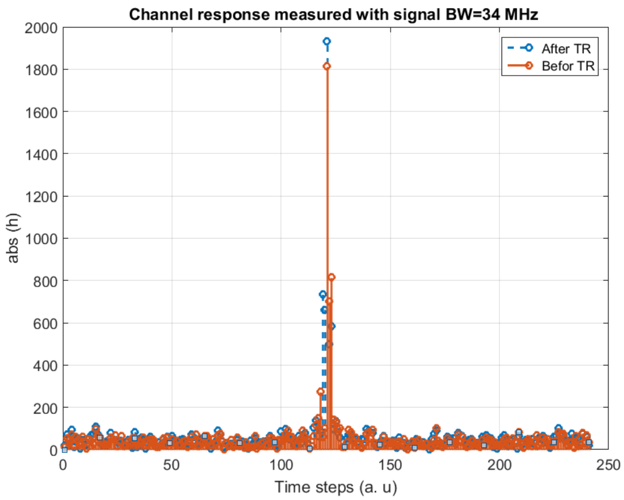

Fig. 5. Cross correlation functions between the transmitted and the received signal at RX_1 with and without TR using a 34MHz sounding signal for channel estimation.

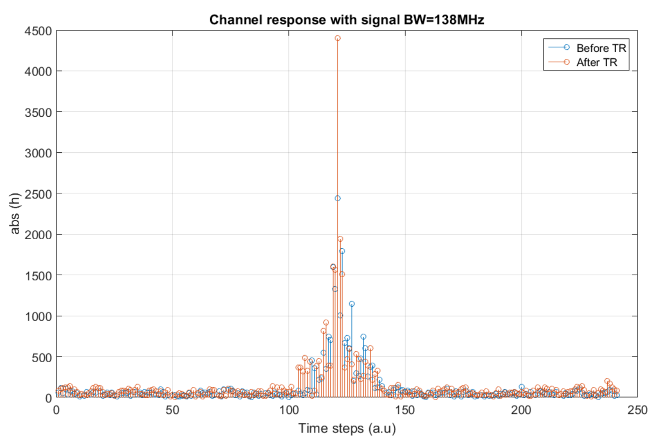

Fig. 6. Cross correlation functions between the transmitted and the received signal at RX_1 with and without TR using a 138MHz sounding signal for channel estimation.

spatiotemporal focusing, when there exists rich multipath and increased bandwidth (more than 100MHz in all our results) for high time resolution CIR estimation.

5. COVERAGE EXTENSION RESULTS

In this section, we introduce our experimental results for signal coverage extension using TR modulation. The increased spatial focusing capability offered by TR, when applied in rich multipath channels, permits the transmitted signal energy to be harvested at desired locations, while reducing power leakage to undesired ones. This power leakage reduction can be exploited in reducing the transmitted power for reaching a desired signal level at a desired location. In other words, TR has the potential of being beneficial for increasing the coverage area for a given transmit power level.

We have considered only RX_1 in the system set up of Fig.(1) and measured the received power in dBm at its antenna element with and without TR modulation. We have used a RF power meter for those RF measurements. We also note that when the received signal passes through the LNA, 10dBm improvement in the received power values will take place. Table 1 includes the obtained powers at RX_1's antenna for different values for the bandwidth of the channel training signal. It is shown from this table that, when using more than 100MHz bandwidth sounding, the received power when applying TR is 4dB stronger compared to the case without TR. However, for the signal bandwidth values 20MHz and 50MHz, the impact of TR modulation is negligible. This implies that, in such cases, the CIR estimation process has reduced time resolvability, and therefore, falls short in exploiting the possible multipath richness of the wireless channel.

Bandwidth	Power without TR	Power with TR
20MHz	-69.0	-69.0
50MHz	-69.5	-68.5
100MHz	-69.0	-66.0
150MHz	-69.0	-65.3
300MHz	-68.5	-65.0
600MHz	-71.0	-67.0

Table 1. Received power in dBm at the antenna of RX_1 with and without TR versus different values for the bandwidth of the channel sounding signal.

6. CONCLUSION

In this paper, we have presented experimental results from our laboratory TR demonstration at 3.5GHz using channel sounding signals covering up to 600MHz bandwidth. Wireless communication based on TR has been lately considered as a promising signal processing technique that can profit from rich multipath radio propagation to provide high resolution spatiotemporal focusing, even with single antenna terminals. Our performance evaluation results in an indoor environment have shown that, for channels with at least 10 strong multipath components and more than 100MHz channel sounding, TR provides less than 5cm spatiotemporal focusing and up to 4dB signal coverage improvement. For future work, we intend to apply TR with multi-antenna transmission considering carrier aggregation. Another interesting research direction is the adoption of reconfigurable and intelligent surfaces [13, 14] for artificially enriching the channel's multipath profile in order to apply TR, and this direction's performance comparison with communication based on Orthogonal Frequency Division Multiplexing (OFDM).

7. REFERENCES

[1] F. Boccardi, R. W. Heath, Jr., A. Lozano, T. L. Marzetta, and P. Popovski, "Five disruptive technology directions for 5G," *IEEE Commun. Mag.*, vol. 52, no. 2, pp. 74–80, Feb. 2014.

[2] J. G. Andrews, S. Buzzi, W. Choi, S. V. Hanly, A. Lozano, A. C. K. Soong, and J. C. Zhang, "What will 5G be?" *IEEE J. Sel. Areas Commun.*, vol. 32, no. 6, pp. 1065–1082, Jun. 2014.

[3] 3GPP, "Study on New Radio (NR) Access Technology-Physical Layer Aspects- Release 14," TR 38.802, 2017.

[4] M. Shafi, A. F. Molisch, P. J. Smith, T. Haustein, P. Zhu, P. D. Silva, F. Tufvesson, A. Benjebbour, and G. Wunder, "5G: A tutorial overview of standards, trials, challenges, deployment, and practice," *IEEE J. Sel. Areas Commun.*, vol. 35, no. 6, pp. 1201–1221, Jun. 2017.

[5] M. Fink, "Time reversal of ultrasonic fields. Part I: Basic principles," *IEEE Trans. Ultrason. Ferroelectron. Frequency Contr.*, vol. 39, pp. 555–566, Sep. 1992.

[6] Y. Chen, B. Wang, Y. Han, H.-Q. Lai, Z. Safar, and K. J. R. Liu, "Why time reversal for future 5G wireless?" *IEEE Signal Process. Mag.*, vol. 33, no. 2, pp. 17–26, Mar. 2016.

[7] G. Lerosey, J. de Rosny, A. Tourin, A. Derode, G. Montaldo, and M. Fink, "Time reversal of electromagnetic waves," *Physical Review Lett.*, vol. 92, no. 19, pp. 1–3, 2004.

[8] R. C. Qiu, J. Q. Zhang, and N. Guo, "Detection of physics-based ultra-wideband signals using generalized RAKE with multiuser detection (MUD) and time-reversal mirror," *IEEE J. Sel. Areas Commun.*, vol. 24, no. 4, pp. 724–730, Apr. 2006.

[9] R. C. Qiu, C. Zhou, N. Guo, and J. Q. Zhang, "Time reversal with MISO for ultrawideband communications: Experimental results," *IEEE Ant. Wireless Prop. Lett.*, vol. 5, pp. 1–5, 2006.

[10] Y. Song, N. Guo, and R. C. Qiu, "Implementation of UWB MIMO time-reversal radio testbed," *IEEE Ant. Wireless Prop. Lett.*, vol. 10, pp. 796–799, 2011.

[11] F. Han, Y.-H. Yang, B. Wang, Y. Wu, and K. J. R. Liu, "Time-reversal division multiple access over multi-path channels," *IEEE Trans. Commun.*, vol. 60, no. 7, pp. 1953–1965, 2012.

[12] B. M. Popovic, "Spreading sequences for multicarrier cdma systems," *IEEE Trans. Commun.*, vol. 47, no. 6, pp. 918–926, 1999.

[13] J. de Rosny, G. Lerosey, and M. Fink, "Theory of electromagnetic time-reversal mirrors," *IEEE Trans. Ant. Prop.*, vol. 58, no. 10, pp. 3139–3149, 2010.

[14] C. Huang, G. C. Alexandropoulos, A. Zappone, M. Debbah, and C. Yuen, "Energy efficient multi-user MISO communication using low resolution large intelligent surfaces," in *Proc. IEEE GLOBECOM*, Abu Dhabi, UAE, Dec. 2018, pp. 1–6.